Published online 18 January 2008 *Nucleic Acids Research, 2008, Vol. 36, No. 5* ***1497–1507***
doi:10.1093/nar/gkm1179

rRNA mutants in the yeast peptidyltransferase center reveal allosteric information networks and mechanisms of drug resistance

Rasa Rakauskaitė and Jonathan D. Dinman*

Department of Cell Biology and Molecular Genetics, University of Maryland, 2135 Microbiology Building, College Park, MD 20742, USA

Received November 27, 2007; Revised December 24, 2007; Accepted December 26, 2007

ABSTRACT

To ensure accurate and rapid protein synthesis, nearby and distantly located functional regions of the ribosome must dynamically communicate and coordinate with one another through a series of information exchange networks. The ribosome is ~2/3 rRNA and information should pass mostly through this medium. Here, two viable mutants located in the peptidyltransferase center (PTC) of yeast ribosomes were created using a yeast genetic system that enables stable production of ribosomes containing only mutant rRNAs. The specific mutants were C2820U (*Escherichia coli* C2452) and Ψ2922C (*E. coli* U2554). Biochemical and genetic analyses of these mutants suggest that they may trap the PTC in the 'open' or aa-tRNA bound conformation, decreasing peptidyl-tRNA binding. We suggest that these structural changes are manifested at the biological level by affecting large ribosomal subunit biogenesis, ribosomal subunit joining during initiation, susceptibility/resistance to peptidyltransferase inhibitors, and the ability of ribosomes to properly decode termination codons. These studies also add to our understanding of how information is transmitted both locally and over long distances through allosteric networks of rRNA–rRNA and rRNA–protein interactions.

INTRODUCTION

The ribosome is a complex nanomachine that accurately converts genetically encoded information into proteins. Given its central role in the life of the cell, the ribosome was a focus of intense study early in the modern age of biochemistry and molecular biology (1). Early chemical analyses revealed that it was mostly composed of RNA, and later biochemical studies suggested that its core functions were RNA mediated (2), a view that has been more recently confirmed by the availability of atomic resolution X-ray crystal structures (3–6). These structures have engendered a renaissance in the field, providing −3D context to heretofore −2D rRNA interaction maps, and frameworks upon which some of the dynamic features of the ribosome can be computationally simulated (7,8).

The ribosome is extremely complex and translation is a highly dynamic process. Different regions of the molecule must coordinate their functions with one another so as to assume the proper conformational states in order to interact with diverse sets of ligands through different stages of the translational program. In addition to X-ray crystallographic, cryo-electron microscopy and molecular dynamics modeling, other approaches are currently being used to understand the dynamics of protein translation. For example, FRET-based approaches provide means to measure changes in distance between various structural elements, providing time resolved views of the moving parts of the machine (9). Chemical footprinting methods allow changes in the sites of interaction between rRNA bases and transacting factors to be mapped over time (10). Combined molecular genetic and biochemical approaches have also been instrumental in understanding ribosome dynamics, revealing such aspects as the kinetic parameters governing translation (11), the role of tRNA conformation in ensuring translational fidelity (12), and potential long range information conduits through the ribosome (13–16).

To ensure that cells are able to synthesize the large quantities of ribosomes required for protein synthesis (17), genomes contain multiple copies of the genes encoding rRNAs, and they are transcribed separately from genes encoding proteins in eukaryotes. This has complicated genetic and biochemical analyses of mutant rRNAs. In prokaryotes, this problem has been bypassed by expressing and purifying aptamer-tagged rRNAs (13,18), by reconstituting ribosomes using synthetic mutant rRNAs, and by synthesizing RNA/DNA hybrid rRNAs (19–23). Unfortunately, similar approaches have not been

*To whom correspondence should be addressed. Tel: +1 301 405 0918; Fax: +1 301 314 9489; Email: dinman@umd.edu

© 2008 The Author(s)
This is an Open Access article distributed under the terms of the Creative Commons Attribution Non-Commercial License (http://creativecommons.org/licenses/by-nc/2.0/uk/) which permits unrestricted non-commercial use, distribution, and reproduction in any medium, provided the original work is properly cited.

successful in eukaryotic systems. Alternatively a genetic strategy used to confront these obstacles has been the construction of *Escherichia coli* and yeast strains lacking chromosomal copies of rDNA genes, allowing episomal expression of pure populations of ribosomes containing mutant rRNAs (24,25). The current study was founded on a previously described method that was used to construct yeast strains stably expressing only mutant rRNAs (15). Here, an improvement of this method was employed to generate rRNA mutants in the peptidyltransferase center (PTC). A complementary series of biochemical and genetic analyses were employed to address questions regarding how the ribosome structure influences its function. These include how structural changes affect ribosome biogenesis and subunit joining during initiation; how they can confer susceptibility/resistance to peptidyltransferase inhibitors; and how ribosomes to properly decode termination codons. In addition, the ribosome is a complex and dynamic nanomachine that must coordinate a significant series of functions among a number of different centers. This engenders questions regarding how rRNA–rRNA and rRNA–protein interactions work to ensure accurate local and long-distance information exchange among its many parts. The studies described in the current work begin to address these questions by focusing on two rRNA mutants located in the PTC of the yeast ribosome, specifically C2820U and Ψ2922C (equivalent to C2452U and U2554C in *E. coli*, see Table 1).

MATERIALS AND METHODS

Strains, media, reagents, genetic, and molecular methods

Escherichia coli DH5α strain was used to amplify plasmids and all experiments were performed in yeast strain JD1314 (*MATa ade2–1 ura3–1 trp1–1 his3–11 leu2–3, 112 can1–100 ΔrDNA::his3::hisG* [L-A HN M_1] + pNOY353). This strain is derived from NOY1049 (26), kindly provided by Dr M. Nomura. Yeast media were prepared as described (27), and galactose media contained 2% galactose instead of glucose. Drug concentrations in yeast media were as follows: doxycycline, 10 μg/ml; hygromycin B, 300 μg/ml; anisomycin, 20 μg/ml. Yeast rRNA-containing plasmids were previously described (15,28). pNOY353 (pGAL) is a *TRP1* selectable, 2μ plasmid containing a 5S rRNA gene under control of its endogenous RNA polymerase III promoter, and a 35S pre-rRNA operon under control of the RNA polymerase II driven *GAL7* promoter. pJD694 (pTET) is a *URA3* selectable, 2μ plasmid containing a 5S rRNA gene under control of its endogenous RNA polymerase III promoter, and a 35S pre-rRNA operon under control of the RNA polymerase II driven, tetracycline (doxycycline) repressible TET promoter. pJD180.Trp is a *TRP1* selectable, 2μ vector containing an entire *RDN1* repeat in which both the 35S pre-rRNA operon and 5S rRNA gene are transcribed from their native RNA polymerase I and III promoters, respectively. Mutations in rDNA encoding regions of pJD694 (pTET) and pJD180.TRP were introduced by oligonucleotide site-directed mutagenesis using DNA oligonucleotides from IDT DNA Technologies (Coralville, IA) and the QuikChange II XL Site-Directed Mutagenesis Kit (Stratagene). Oligonucleotide design and reaction conditions were as recommended by the manufacturer. All mutations were confirmed by sequencing. Transformations of yeast strain JD1314 were performed according to alkaline cation protocol (29). Yeast strains expressing mutations in rRNA were selected as previously described (15). To switch rRNA transcription from RNA polymerase II to RNA polymerase I driven transcription of 35S pre-rRNA, yeast strains expressing wild-type or mutant rRNA from pTET were transformed with pJD180. Trp-based plasmids containing either wild-type sequence or the specified mutations in the 25S rDNA gene. Transformants were initially selected on H −Trp −Ura medium, followed by two passages of replica plating onto H −Trp + 5-FOA thus identifying cells in which 35S pre-rRNA was only expressed from the RNA polymerase I promoter. Direct reverse transcriptase primer extension sequence analysis of rRNAs extracted from purified ribosomes was performed as previously described (15).

Table 1. Comparative numbering for bases of large subunit rRNA discussed in the current study

Saccharomyces cerevisiae	*Escherichia coli*	*Haloarcula marismortui*
G2621*	G2252	G2285
A2778	A2407	U2445
A2779	U2408	G2446
G2814*	G2446	G2481
A2818*	A2450	A2485
A2819*	A2451	A2486
C2820*(v)	C2452	C2487
G2822	G2454	G2489
U2825	Ψ2457	U2492
U2828	U2460	U2495
G2862	G2494	G2529
A2863	G2495	C2530
C2866	C2498	C2533
G2921	G2553	G2588
Ψ2922*(v)	U2554	U2589
U2948*	Ψ2580	U2615
A2971*	A2602	A2637
A3047	C2681	C2718
A3048	A2682	A2719

Asterisk denote bases of yeast 25S rRNA targeted for mutagenesis. Bases marked with (v) yielded viable mutants.

Genetic assays

General growth defects were monitored by dilution spot assay in which 2.5 μl of five sets of 10-fold dilutions were spotted on the YPAD medium yielding a range of spots from 10^5 to 10^1 CFU/spot. Plates were incubated at 18°C, 30°C, and 37°C. For drug disc assays, 10 μl solutions containing 7.8 μg/ml sparsomycin, 2 μg/ml anisomycin or 250 μg/ml paromomycin were applied to 6 mm diameter filter paper discs and air dried. Overnight yeast cultures were diluted to $OD_{595} = 0.3$, 300 μl of the resulting suspensions were plated onto YPAD medium, the drug-saturated discs were applied, plates were incubated at 30°C for 3 days and the diameters of growth inhibition zones were measured. A minimum of at least two

independent assays was employed. The ability of cells to suppress a UAA nonsense codon utilized the pYDL-UAA dual luciferase reporter constructs as previously described (30). At least 9–12 readings were taken for each sample until the data were normally distributed to enable statistical analyses both within and between experiments (31). The [PSI^+] prion form of yeast eukaryotic release factor 3 (eRF3) was cured after several passages of cells on YPAD media containing 5 μg/ml of guanidinium hydrochloride (32). Cured strains were transformed with the pYDL-UAA reporter constructs and analyzed as described above.

Aminoacyl-tRNA binding assays, polysome profiles, rRNA chemical protection, and molecular visualization

Yeast phenylalanyl-tRNA was purchased from Sigma (St Louis, MO), charged with [^{14}C]-Phe or Ac-[^{14}C]-Phe and purified by HPLC as previously described (33). Ribosomes were isolated from isogenic wild-type and mutant cells, and tRNA-binding studies were carried out as previously described (33). Lysates of cycloheximide arrested yeast cells were sedimented through 7–47% sucrose gradients and polysome profiles were determined by monitoring A_{254} nm as previously described (34). Purified ribosomes were pre-incubated with 100-fold molar excess of anisomycin or buffer, chemically probed with dimethylsulphate (DMS), kethoxal or carbodiimide metho-*p*-toluenesulfonate (CMCT), followed by reverse transcriptase primer extension analyses of modified rRNAs as previously described (35) with the modification that reactions were performed at 30°C instead of 37°C. The following primers were used: 25-4 (5′-TAAAGGATCGATAGGCC-3′); 25-5 (5′-GTCGCTATGAACGCTTG-3′); 25-6 (5′-AACCTGTCTCACGACGG-3′); 25-7 (5′-CCTGATCAGACAGCCGC-3′); 25-8 (5′-GACGCCTTATTCGTATCCA-3′); 25-10 (5′-GGTATGATAGGAAGAGC-3′); and 25-11 (5′-CCTCTATGTCTCTTCAC-3′). Primer extensions from 25-4 allowed analyses spanning helices 83–87; 25-5 covered bases in the PTC and in helixes 86–88; 25-6 enabled analysis of helices 89–93; 25-7 covered bases from helices 93 to 95; 25-8 covered helixes 96–97, 25-10 covered helix 89 of 25S rRNA, and 25-11 covered helices 73–74 of 25S rRNA. X-ray crystal structures of the *Haloarcula marismortui* 50S ribosomal subunit complexed with either anisomycin (PDB IK73) (36) or with CCA-Phe (PDB 1VQ6) (8) were visualized using PyMOL (DeLano Scientific LLC).

RESULTS

Generation of rRNA mutants in the PTC and the A-loop

Previously, we described a genetic protocol enabling construction of yeast cells stably expressing only mutant rRNA alleles (15). In the first phase of the current study, this method was applied to selected bases of 25S rRNA. Bases were chosen for mutagenesis because of their locations in or near important structural elements of the PTC and because mutations at these positions had been previously shown to promote altered sensitivities to antibiotics in various prokaryotes and archae (36). Yeast 25S rRNA bases targeted for mutagenesis, and their corresponding 23S rRNA bases in *E. coli* and *H. marismortui* are shown in Figure 1A and B and Table 1. For consistency, the yeast numbering system is primarily used throughout this report. Mutagenesis of G2621 (the 'P-loop'), G2814, A2818, A2819, U2947, and A2971 (all in the core of the PTC) to any of the three alternative bases were inviable, supporting the prior observation of a quality-control mechanism capable of detecting and eliminating the defective rRNAs in ribosomes (37). Two alleles did prove to be viable: cytosine 2820 to uracil (C2820U), and pseudouridine 2922 to cytosine (Ψ2922C) (Figure 1A and B). The C2820A mutant was also viable, but only in the presence of high concentrations of anisomycin, i.e. it was anisomycin-dependent for growth (Figure 1D).

In the course of these studies, it was observed that cells expressing wild-type rRNA from either the pGAL or pTET plasmids (RNA polymerase II promoters) were intrinsically temperature sensitive and grew at significantly slower rates than cells in which the wild-type rRNA was transcribed from the native RNA polymerase I promoter (e.g. the pJD180 series of plasmids). This is consistent with the observation that transcription of 35S pre-rRNA by RNA polymerase II is suboptimal for cell growth and viability, perhaps introducing an unwanted set of artifacts into the system (38–40). To address this, cells expressing either the wild-type rRNA sequence, or those expressing only the C2820U or Ψ2922C forms of 25S rRNA using the pTET system (RNA Pol II) were transformed with plasmids in which 35S pre-rRNA is transcribed from the native RNA polymerase I promoter (pJD180.Trp). Standard plasmid shuffle methods (41) were then used to obtain cells expressing either wild-type or mutant 35S rRNAs. These cells were significantly more robust (data not shown).

Improvement of the genetic system enabled more fine scale analyses of the effects of the two mutants on cell growth. C2820U conferred strong temperature (37°C) and cold (18°C) sensitive growth defects (Figure 1C) and resistance to anisomycin (Figure 1D), a competitive inhibitor of aa-tRNA binding (42). The C2820A mutant was also viable, but only in the presence of high concentrations of anisomycin, i.e. it was anisomycin-dependent for growth (Figure 1D). Even under these conditions however, it did not grow well, and we were unable to perform subsequent analyses with this allele. C2820G was inviable. Ψ2922C, located at the tip of helix 92 (the A-loop) resulted in slightly decreased growth at 37°C and cold sensitivity (Figure 1C). The Ψ2922A and Ψ2922G promoted mutants were inviable as the sole forms of 25S rRNA.

The C2820U and Ψ2922C 25S rRNA mutants affect large subunit biogenesis

Mutations of 60S components often promote large ribosomal subunit biogenesis defects. Sucrose density gradient analysis of cycloheximide arrested S30 cytosolic preparations (polysome profiles) revealed significant differences between wild-type and mutant rRNAs (Figure 1E). The 60S/40S ratio >1 observed when

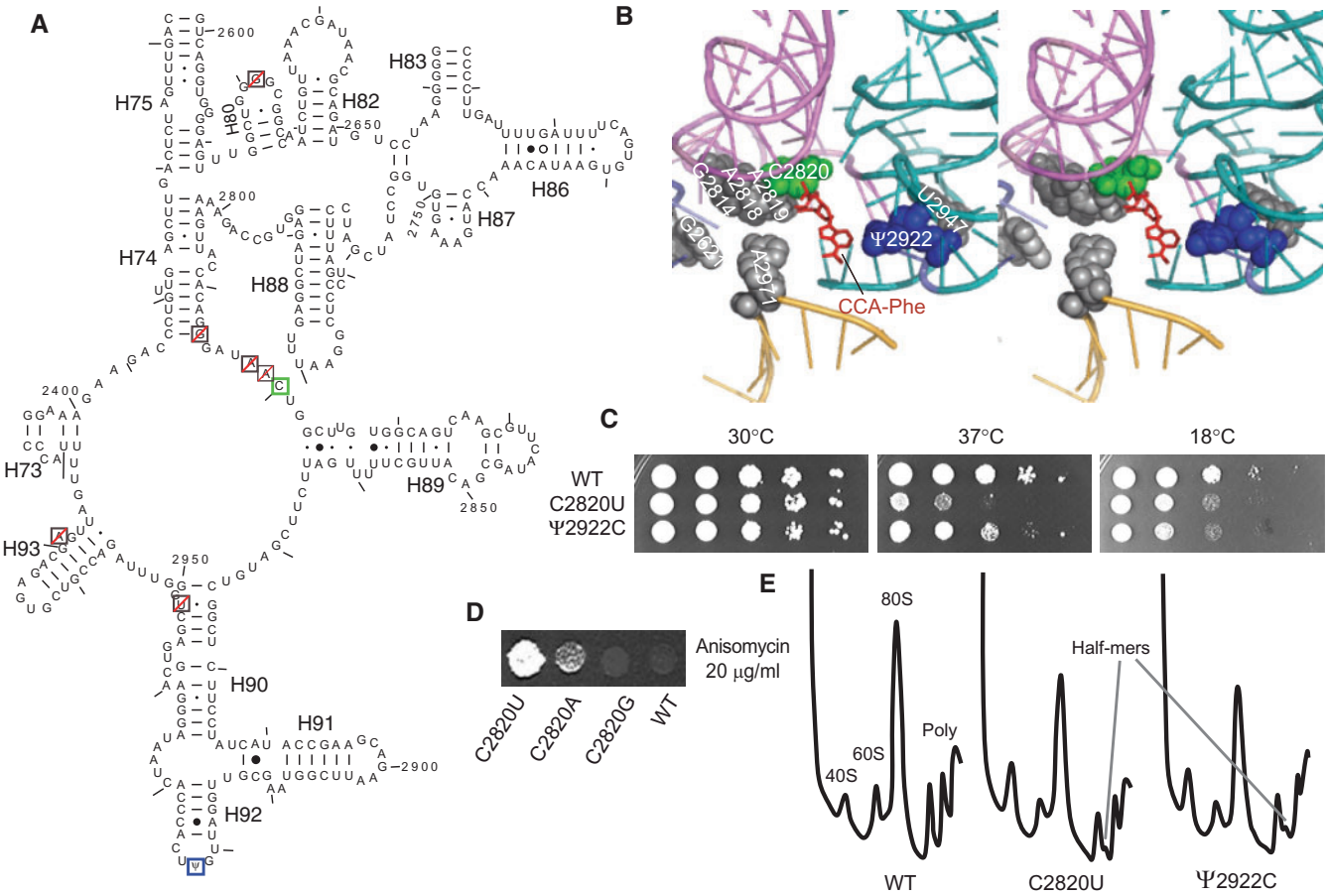

Figure 1. Generation and preliminary characterization of mutants in the yeast peptidyltransferase center (PTC). (**A**) 2D map showing locations of bases in the PTC targeted for mutagenesis. All alleles of bases boxed in black with red diagonal slashes were inviable as the sole forms of 25S rRNA. Bases for which viable mutants were obtained are boxed in green (C2820U) and blue (Ψ2922C). This color scheme is used throughout the figures. (**B**) 3D stereoscopic view of the mutants mapped in panel A based on the *Haloarcula marismortui* atomic resolution 50S structure (8). The location of Phe-ACC in the A-site of the PTC is shown in red. (**C**) Dilution spot assays of the effects of the two viable mutants expressed as the sole forms of 25S rRNA from the native RNA polymerase I promoter on cell growth at optimum (30°C), high (37°C), and low (18°C) temperatures. (**D**) Growth phenotypes of C2820 mutants in the presence of anisomycin. Primary transformants were grown on −trp medium containing 5-FOA to select against wild-type rRNA, hygromycin to select for mutant rRNA, and 20 μg/ml anisomycin. Note that C2820A was only viable in the presence of anisomycin. (**E**) 60S ribosomal subunit biogenesis and polysome defects caused by expression of C2820U or Ψ2922C mutations transcribed from the native RNA polymerase I promoter. Cytoplasmic extracts from isogenic strains were separated through continuous 7–47% sucrose gradients in an SW41 rotor at 40,000 r.p.m. for 240 min at 4°C, and analyzed by continuous monitoring of A_{254}. Positions of 40S, 60S, 80S, polysomes, and half-mers are indicated.

wild-type rRNA was episomally expressed from the native RNA polymerase I promoter was similar to the pattern observed using 'wild-type' cells where rRNAs are transcribed from the native, chromosomal context. Episomal expression of the C2820U and Ψ2922C mutants using this system revealed 60S/40S ratios of <1, decreased 80S peak heights, and the presence of half-mer polysomes. These observations are suggestive of defects in 60S subunit biogenesis and in translation initiation. As discussed below, this defect may be occurring at the stage of 60S joining with the 43S pre-initiation complex.

The effects of C2820U on rRNA structure are locally confined, while Ψ2922C affects both local and distant rRNA structures

Given the large subunit-specific effects of the mutants, chemical protection methods were used to probe for effects of the mutants on 25S rRNA structure. Ribosomes purified from wild-type and mutant cells were pre-incubated with 100-fold molar excess of anisomycin or in buffer alone, and subsequently probed for structural changes using three base-specific solvent accessible reagents: DMS, kethoxal, and CMCT. rRNAs were extracted, and modified bases were identified by primer extension using reverse transcriptase to detect methylation at the N3 position of uridines and the N1 position of guanosines (CMCT), at the N1 and N2 positions of guanosines (kethoxal), and at the N1 position of adenosines and N3 position of cytidines (DMS) (43). Reverse transcriptase cannot use modified bases as templates for cDNA synthesis, resulting in strong stops one base 5′ of the site of modification. The reverse transcriptase reactions were also scored for changes in 'in-line cleavage' patterns as caused by alterations in the flexibility of bases in

single-stranded regions of RNA, which can affect the frequency of spontaneous cleavage of an RNA phosphodiester linkage via an internal nucleophillic attack by the 2′ oxygen on the adjacent phosphorous center (44). These appear as increased or decreased band intensities at the site of the cleavage due to runoff of the enzyme. The primers used (see Materials and Methods) were designed to probe functional regions of domain V (including the A-site and P-site loops, the PTC, and the helices adjacent to these structures, i.e. helices 73, 74, 89–93) and helices 94–96.

The results of these experiments are shown in Figure 2. In general, the effects of the C2820U mutant were localized to the vicinity of the lesion in 25S rRNA at the base of helix 89. Specifically, this mutation promoted hyperprotection (i.e. decreased solvent accessibility) of G2862 to chemical attack (Figure 2A and B, open triangle). G2822 and U2825 were also hyperprotected both in the presence and absence of chemical agent, a pattern that is indicative of in-line cleavage (indicated by arrows in Figure 2A and B). The increased protection of U2825 from in-line cleavage and of G2862 from chemical attack suggests that this base pair is strengthened by the C2820U mutation.

The effects of the Ψ2922C mutation on 25S rRNA structure were more widely distributed and generally led to increased exposure of affected bases to solvent (Figure 2A and C). At the site of the mutation, the cytosine at position 2922 became deprotected. Locally, the in-line cleavage patterns of two bases, G2921 (decreased reactivity) and U2948 (increased reactivity) were also observed. The Ψ2922C mutation also specifically promoted deprotection of two clusters of adjacent adenosine residues in distal regions of 25S rRNA. In the loop of helix 88 (the E-site), this mutation promoted deprotection of A2778 and A2779. Similarly, A3047 and A3048, which map to a bulge in helix 96 were also deprotected.

Comparison of rRNAs in the presence or absence of anisomycin was also informative. In wild-type (and Ψ2922C) cells, addition of anisomycin resulted in protection of C2820 from chemical attack as compared to the no-drug controls (Figure 2C, indicated by white versus black triangles, respectively). These data are consistent with a prior study showing that anisomycin protected this cytosine in the yeast 25S rRNA from chemical attack (45). In contrast, anisomycin did not alter the protection pattern at the C2820U mutant (indicated by circles in Figure 2C), suggesting that the drug does not interact with this base. This is consistent with studies of anisomycin resistant *Halobacterium* and *Thermophilus* species containing C to U mutations at this position (36,45).

C2820U and Ψ2922C affect tRNA binding to the ribosomal P-site

Changes in rRNA structure in the vicinity of the PTC can affect tRNA binding. To test for such effects, tRNA-binding assays were performed under equilibrium conditions. To monitor tRNA binding to the A-site, non-salt washed ribosomes were first incubated with excess unlabeled deacylated tRNA to block non-specific binding sites, and subsequently with increasing concentrations of [^{14}C] Phe-tRNA (aa-tRNA). These conditions result in eEF1A assisted binding of labeled aa-tRNA to the A-site. These studies indicated that neither of the mutants affected A-site tRNA binding (Figure 3A and B). To monitor binding to the P-site, purified ribosomes were incubated in increasing concentrations of acetylated [^{14}C] Phe-tRNA (Ac-aa-tRNA), which specifically has high affinity for the P-site. These experiments demonstrated that the mutants promoted more than two-fold increases in the dissociation constants (K_d) for tRNA at the ribosomal P-site (Figure 3C and D).

The C2820U and Ψ2922C mutants promote hypersensitivity to sparsomycin and paromomycin and affect termination codon recognition in the presence of the [*PSI*$^+$] prion

tRNA-binding defects are often accompanied by hypersensitivity to translational inhibitors. Filter disc assays confirmed that C2820U was resistant to anisomycin as indicated by the lack of a zone of growth inhibition around the anisomycin disc (Figure 4A). Sparsomycin interacts with the P-site and affects interactions between the ribosome and the peptidyl-tRNA (36,46). Consistent with the changes in K_d values for Ac-aa-tRNA, increases in the zones of growth inhibition around the sparsomycin discs showed that both mutants were hypersensitive to this drug relative to wild-type cells (Figure 4A). With regard to the Ψ2922C mutant, this is consistent with a prior report showing that deletion of *snr10*, the snoRNA that directs pseudouridylation of U2922 also promoted sparsomycin sensitivity (47). Although paromomycin is an aminoglycoside antibiotic that interacts with the decoding center in the small subunit (48), mutations of large subunit rRNAs and proteins have been previously shown to affect sensitivity to this drug (49–51). The very large growth inhibition zones promoted by paromomycin indicated that both mutants were hypersensitive to this antibiotic (Figure 4A), also consistent with paromomycin hypersensitivity of the *snr10Δ* mutant (52). Paromomycin stimulates termination suppression in yeast (53). Thus, the effects of the two mutants on the ability of ribosomes to recognize the UAA termination codon was assayed using a previously described dual-luciferase reporter system (54). The results demonstrated that the C2820U mutant slightly stimulated translational suppression of the UAA codon, while Ψ2922C was approximately two-fold more accurate (Figure 4B). The actual rates of UAA suppression originally observed in wild-type cells (4.5%) was unusually high however, commensurate with levels normally associated with the presence of [*PSI*$^+$] (30), the prion form of yeast eRF3 (55). To test this hypothesis and to examine the effects of termination suppression in the absence of the prion, cells were cured of [*PSI*$^+$] by serial passage in the presence of guanidinium hydrochloride (32). In wild-type cells, this treatment returned rates of UAA suppression down to normal levels (0.27%) (Figure 4B, see inset). Interestingly, the mutants no longer affected termination suppression when cured of [*PSI*$^+$].

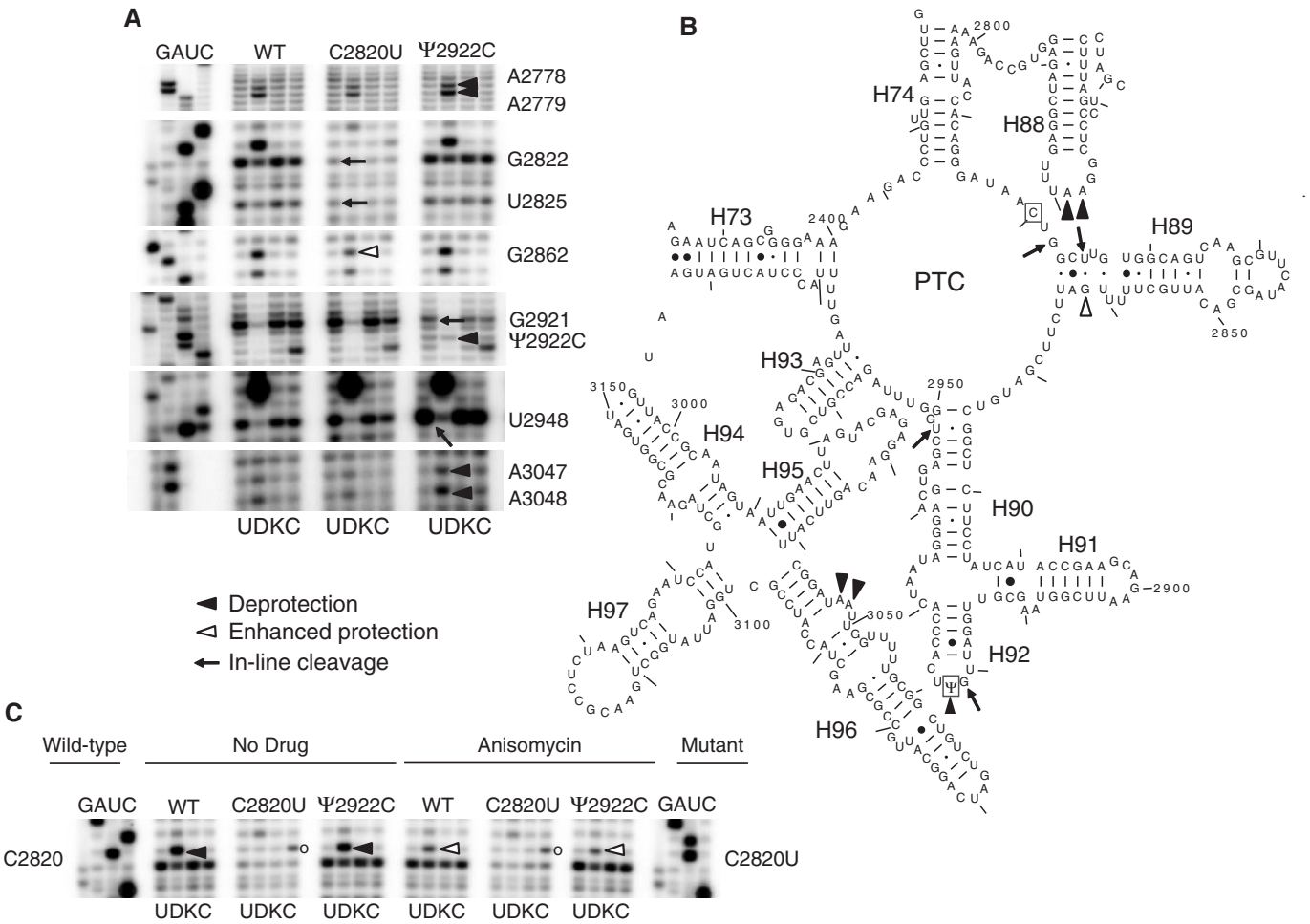

Figure 2. rRNA structural analyses. (**A**) Structure probing of wild-type and mutant ribosomes through helices 88–97. Sequencing ladders (left) and primer extensions were generated with AMV reverse transcriptase using rRNAs isolated from purified ribosomes. Along the bottom, U indicates untreated samples; D denotes ribosomes treated *in vitro* with dimethylsulphate (DMS); K is ribosomes treated *in vitro* with kethoxal; C designates ribosomes treated *in vitro* with carbodiimide metho-*p*-toluenesulfonate (CMCT). Individual nucleotide positions of bases in mutant samples showing altered protection patterns are indicated along the right side. Enhanced chemical protection relative to wild-type rRNA are indicated by white triangles, and bases showing relative deprotection are indicated by black triangles. Note that base modification inhibits recognition by reverse transcriptase, resulting in strong stops one nucleotide 5′ of the chemically modified base. Bases with altered in line rRNA cleavage patterns are indicated by black arrows. Note that in-line cleavage results in transcriptional runoff by reverse transcriptase producing an intense band at the site of cleavage. (**B**) 2D mapping of data shown in panel A. Sites of the mutations are boxed as in Figure 1A. Labeling follows conventions described in Panel A. PTC denotes the peptidyltransferase center. Helices are numbered, the locations of every 50th base are numbered from the 5′ end of yeast 25S rRNA, and every 10th base is indicated by tick marks. (**C**) Effects of anisomycin on chemical modification. As indicated, ribosomes were pre-incubated in 100-fold molar excess of anisomycin, or without drug. Circles denote CMCT reactivity of U2820 in the C2820U mutant. Sequence ladder of C2820U mutant is shown at right.

This suggests that the mutants only affect UAA recognition when eRF3 availability is limited.

DISCUSSION

The current study employed a genetic method to create rRNA mutants targeted to the PTC. Almost all of the mutants were inviable as the sole forms of large subunit rRNA in agreement with prior studies in *E. coli* (see Refs. 56–59). Unlike bacteria, where an *in vitro* ribosome reconstitution (60), and the ability to affinity purify tagged ribosomes (59,61) has enabled biochemical characterization of such inviable mutants, similar studies of eukaryotic ribosomes are hampered by the lack of these tools. Despite these limitations, two viable mutants, C2820U and Ψ2922C, were generated in yeast and characterized using biophysical, biochemical and genetic methods. This discussion focuses on how the data so gathered add to our understanding of how the structure of the ribosome influences its function.

Local changes in the PTC

As noted above, the ribosome has a many functional centers and moving parts whose activities must be coordinated throughout the different phases of translation. Cryo-electron microscopy reconstructions have revealed large-scale rearrangements between and within both large and small subunits during different phases

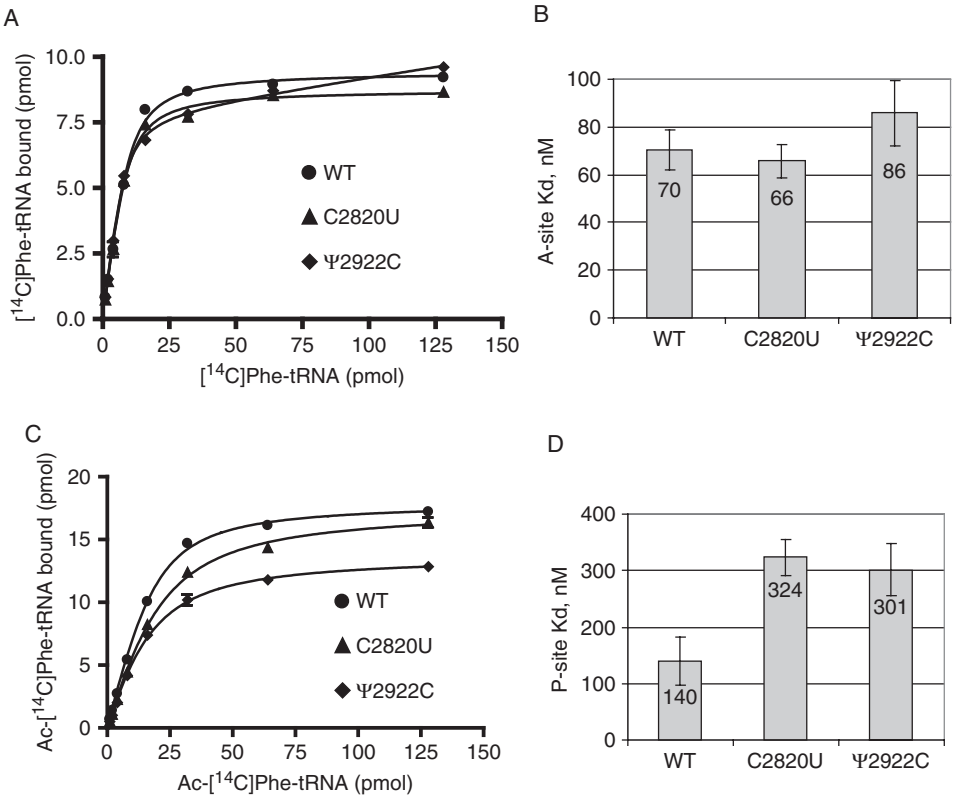

Figure 3. tRNA-binding studies. Binding of aminoacyl-tRNA to the ribosomal A-site (panels **A** and **B**), or of acetylated-aa-tRNA to the P-site was carried out in 30 µl reaction mixtures containing 25 pmol of ribosomes primed with 25 µg of poly(U). For A-site binding assays, non-salt washed ribosomes were preincubated with 10 µg uncharged tRNAs at 30°C for 30 min to insure full occupation of P-sites by uncharged tRNA. Increasing amounts (1–128 pmol) of [^{14}C]-Phe-tRNA were added, and incubations continued for 20 min at 30°C to allow formation of [^{14}C]-Phe-tRNA·80S·poly(U). To monitor P-site binding, salt-washed ribosomes were incubated at 30°C for 20 min with increasing amounts (1–128 pmol) of Ac-[^{14}C]-Phe-tRNA. Reaction mixtures were applied onto nitrocellulose membranes, filters were washed with binding buffer, and radioactivity was measured by scintillation counting. Single site-binding isotherms were fitted to the data (panels A and **C**) and K_d values (panels B and **D**) were calculated using GraphPad Prism 4.

of translation, suggesting pathways for signal transduction over long distances (62). The highly conserved nature of the rRNA residues examined and identified in this study allows them to be mapped to atomic-resolution ribosome structures with a relatively high degree of confidence. Thus, the mutants and bases with altered reactivity were mapped to the *H. marismortui* 50S atomic resolution structure (Figure 5). The rationales for using this structure are (i) it represents the highest resolution large subunit structure available and (ii) both the bases that were mutagenized and those whose protection patterns were altered are highly conserved and are found in structurally conserved, core regions of the ribosome.

Figure 5A shows a 'big picture' view of where the bases identified in Figure 2 map to the large subunit 3D structure. A close-up view shows that both the C2820U and Ψ2922C mutants affected local rRNA structures at the PTC proximal ends of the helix 89 and the helix 90–92 structure, respectively (Figure 5B). These form the two sides of the aa-tRNA accommodation corridor at the A-site of the PTC (7). C2820U promoted hyperprotection and/or decreased flexibility of the helix 89 side of this structure by stabilizing the U2825–G2862 base pair, and restricting the flexibility of G2822. In contrast, the Ψ2922C mutant resulted in deprotection/altered flexibility of key residues on the other side of the corridor, G2921 and U2948. Consistent with the induced fit model of peptidyltransfer (8), we suggest that the combination of the weak base pairing potential at the base of helix 89 in combination with the inherent flexibility at the base of the helix 90–92 structure work together to properly configure the A-site region of the PTC depending on tRNA occupancy status. We hypothesize that these mutants have shifted the dynamic nature of this region toward the conformation favored by the presence of aa-tRNA in the A-site, i.e. the 'open' conformation of the A-site crevice (8,63,64).

To account for the specific effects observed on binding of Ac-aa-tRNA to the P-site but not of aa-tRNA to the A-site, it is important to note that the assay for A-site binding was performed in excess of cold deacylated tRNA because the aa-tRNA alone can bind equally well to either site. Thus, full occupancy of both the A- and P-sites in the PTC in this assay could help to stabilize and maintain the labeled aa-tRNA in the correct orientation, resulting in no apparent effects on aa-tRNA binding. In contrast, because of its highly specific affinity for P-site, only Ac-[^{14}C]Phe-tRNA is used in the P-site binding assay.

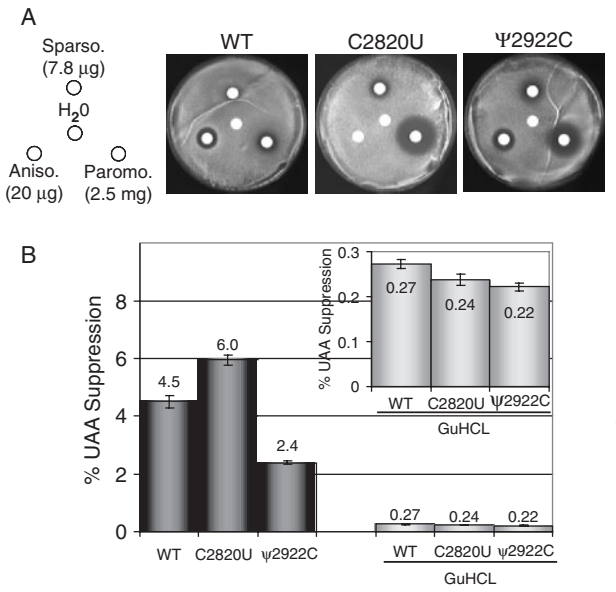

Figure 4. Phenotypic analyses of C2820U and Ψ2922C mutants. (**A**) Drug disc assays. Overnight yeast cultures were diluted to OD_{595} = 0.3, and 300 µl of the resulting suspensions were plated onto rich medium. Sterile 0.6 cm diameter filter paper discs were saturated with the indicated amounts of sparsomycin, anisomycin, paromomycin or water and placed onto the plates. Cells were incubated at 30°C for 3 days and the diameters of growth inhibition zones were monitored. (**B**) UAA termination suppression assays. Suppression of a UAA nonsense codon utilized the pYDL-UAA dual luciferase reporter constructs as previously described (30,31). The [*PSI*$^+$] prion form of yeast eukaryotic release factor 3 (eRF3) was cured after several passages of cells on YPAD media containing 5 µg/ml of guanidinium hydrochloride (GuHCL). Cured strains were transformed with the pYDL-UAA reporter constructs and analyzed as described above. The insert shows the same data with an expanded Y-axis. Error bars denote standard error.

With no other tRNAs present to stabilize its interactions with the ribosome, binding of the Ac-aa-tRNA would be more sensitive to distortions in the PTC, resulting in the observed increased K_d's of the mutants for Ac-aa-tRNA (Figure 3C and D). Indeed, these mirror actual biological conditions, where the P-site can be occupied by peptidyl-tRNA while the A-site is empty, but the A-site is never occupied by tRNA without the P-site being filled. This may explain why both the C2820U and Ψ2922C mutants were hypersensitive to the P-site specific antibiotic sparsomycin (Figure 4A): the effects of these mutants are most strongly manifested when there is no tRNA present in the A-site to help stabilize the peptidyl-tRNA. We also suggest that decreased affinities for peptidyl-tRNA could be the underlying cause of the 60S subunit joining defects (Figure 1E), as binding of initiator tRNA to the P-site without a tRNA in the A-site is a central event in translation initiation. Lastly, even though a two-fold change in K_d is only ≈100 calories, these results support the notion that small biochemical changes can be amplified through a series of physiological events resulting in significant biological effects.

The chemical protection studies performed in the presence or absence of anisomycin (Figure 2C) confirms that anisomycin protects C2820 from attack by DMS. The hydrophobic *p*-methoxyphenyl group of anisomycin is inserted into the A-site crevice where it aromatically stacks with C2820 (*E. coli* C2452, *H. marismortui* C2487), while the nitrogen of its pyrrolidine group hydrogen bonds with N3 of this base. It is also stabilized by interactions with additional bases and coordination with a potassium ion. The C2820U mutation is predicted to eliminate the hydrogen bond to the pyrrolidine nitrogen atom of anisomycin (36). Our finding that anisomycin failed to change the chemical protection pattern at this site in the C2820U mutant suggests that anisomycin cannot interact with uracil in this position, providing empirical support for this model in a eukaryotic ribosome.

Long-distance information exchange within the large subunit

Although the concept of allosteric information exchange within the ribosome has been known since the linkage between streptomycin and rifampicin mutants were established (65), mapping of specific intraribosomal information exchange networks remains a challenge. Figure 5C shows that the Ψ2922C mutant promoted deprotection of 25S rRNA residues located very far apart from one another. Specifically, A2778 and A2779 are located near the E-site at the tip of the loop of helix 88. This helix is coaxially stacked with helix 74, which in turn contacts the PTC where Ψ2922C is located. Also in this region, this mutation rendered U2948 more susceptible to in-line cleavage, consistent with the 'open' A-site crevice hypothesis. It is also notable that deletion of U2948, or mutating it to G, C, or A resulted in lethality, suggesting that the identity of this base is critical. In the *H. marismortui* crystal structure, this base interacts directly with K226 (yeast K244), which resides in the central extension of ribosomal protein L3 (see Figure 5B and C). At the base of this extension is the major globular domain of L3, six residues of which make extensive hydrogen bond based contacts with A3047 and A3048, the other two residues that were deprotected in the Ψ2922C mutant (Figure 5C and D). These residues are important because they rest at the base of helix 95, atop which sits the Sarcin/Ricin loop, which is involved in elongation factor binding (66). Thus, even though the tip of helix 88 and the base of helix 95 are separated by ~135 Å, the chemical protection analyses reveal a direct line of communication connecting the A-, P-, and E-sites with the elongation factor binding center. These data tie in well with other findings. For example, mutation of T54 (which interacts with A3048, see Figure 5D) to alanine, was identified as promoting resistance to anisomycin (33). Another study of the central extension of ribosomal protein L3 in which K244 resides showed that this domain of the protein functions to communicate and coordinate the various steps of the translation elongation cycle between the PTC and the elongation factor binding site (67), and to fine tune the 3D geometry of the PTC (68). Additionally, the chemical reactivity of these two bases were also affected by mutation of the N-terminal extension of L3, and we have suggested an allosteric model for how L3 functions as part of an allosteric switch to communicate the tRNA

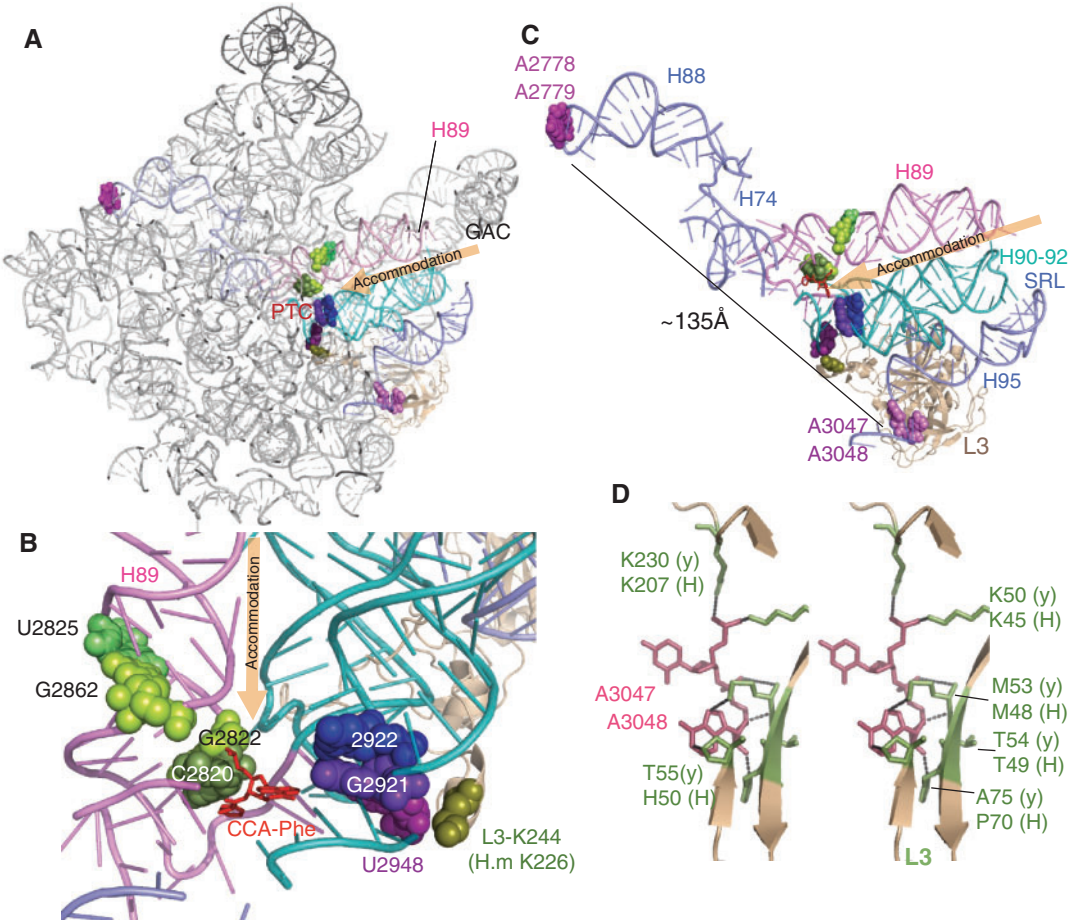

Figure 5. Modeling the effects of the C2820U and Ψ2922C mutants on ribosome structure. Yeast 25S rRNA bases and ribosomal protein L3 were mapped onto atomic resolution structures of the *Haloarcula marismortui* 50S subunit (8). Bases associated with structural changes due to the C2820U mutant are shown in shades of green, while those associated with the Ψ2922C mutant are shown in shades of purple. CCA-Phe is shown in red. (**A**) Crown view of the large subunit. PTC indicates the peptidyltransferase center (PTC), GAC shows the GTPase-associated center. The orange arrow labeled 'accommodation' indicates the path taken by the aa-tRNA 3′ end during the process of accommodation. (**B**) Close-up view of the PTC showing the C2820 and Ψ2922 mutants and nearby bases affected by the two mutants. L3-K244 (H.m. K226) indicates the position of conserved lysine that shares a hydrogen bond with U2948. (**C**) Locations of distal nucleotides affected by the Ψ2922C mutation. Note that this mutant affects two clusters of nucleotides located ~135Å apart, from the E-site (A2778, A2779) to the base of the globular domain of L3 (A3047, A3048). We suggest that this is evidence of a long-distance communication network extending from the E-site down helices 88 and 74 into the PTC, across to the central extension of ribosomal protein L3, down to the L3 globular domain to the base of helix 95 (A3047, A3048). (**D**) Stereoscopic view of interactions between A3047, A3048, and indicated amino acid side chains of ribosomal protein L3.

occupancy status of the PTC to other functional regions of the ribosome (69). The current study allows us to extend this long-distance information conduit out to the E-site, where presumably information pertaining to its occupancy status by deacylated tRNA can be tied into this network. In addition, consistent with our studies of helix 38 (15), the hypersensitivity of the C2820U and Ψ2922C mutants to paromomycin and the effects of these mutants on termination codon recognition (albeit only when eRF3 is limiting due to the presence of the [*PSI*$^+$] prion) points to long-distance communication and coordination of function between the PTC in the large subunit and the decoding center in the small subunit.

ACKNOWLEDGEMENTS

We would like to thank the members of the Dinman laboratory, with special thanks to Arturas Meskauskas, Alexey Petrov, and Michael Rhodin for their support and keen insight. This work was supported by a grant from the Public Health Service to J.D.D. (GM058859). Funding to pay the Open Access publication charges for this article was provided by Public Health Service grant GM058859.

Conflict of interest statement. None declared.

REFERENCES

1. Mathews,M.B., Sonenberg,N. and Hershey,J.W.B. (2007) Origins and principles of translational control. In Mathews,M.B., Sonenberg,N. and Hershey,J.W.B. (eds), *Translational Control in Biology and Medicine*. Cold Spring Harbor Press, Cold Spring Harbor, NY, pp. 1–40.
2. Green,R. and Noller,H.F. (1997) Ribosomes and translation. *Annu. Rev. Biochem.*, **66**, 679–716.
3. Clemons,W.M. Jr, May,J.L., Wimberly,B.T., McCutcheon,J.P., Capel,M.S. and Ramakrishnan,V. (1999) Structure of a bacterial 30S ribosomal subunit at 5.5 Å resolution. *Nature*, **400**, 833–840.

4. Ban,N., Nissen,P., Hansen,J., Moore,P.B. and Steitz,T.A. (2000) The complete atomic structure of the large ribosomal subunit at 2.4 Å resolution. *Science*, **289**, 905–920.
5. Schluenzen,F., Tocilj,A., Zarivach,R., Harms,J., Gluehmann,M., Janell,D., Bashan,A., Bartels,H., Agmon,I. *et al.* (2000) Structure of functionally activated small ribosomal subunit at 3.3 angstroms resolution. *Cell*, **102**, 615–623.
6. Yusupov,M.M., Yusupova,G.Z., Baucom,A., Lieberman,K., Earnest,T.N., Cate,J.H. and Noller,H.F. (2001) Crystal structure of the ribosome at 5.5 Å resolution. *Science*, **292**, 883–896.
7. Sanbonmatsu,K.Y., Joseph,S. and Tung,C.S. (2005) Simulating movement of tRNA into the ribosome during decoding. *Proc. Natl Acad. Sci. USA*, **102**, 15854–15859.
8. Schmeing,T.M., Huang,K.S., Strobel,S.A. and Steitz,T.A. (2005) An induced-fit mechanism to promote peptide bond formation and exclude hydrolysis of peptidyl-tRNA. *Nature*, **438**, 520–524.
9. Vanzi,F., Vladimirov,S., Knudsen,C.R., Goldman,Y.E. and Cooperman,B.S. (2003) Protein synthesis by single ribosomes. *RNA*, **9**, 1174–1179.
10. Unbehaun,A., Marintchev,A., Lomakin,I.B., Didenko,T., Wagner,G., Hellen,C.U. and Pestova,T.V. (2007) Position of eukaryotic initiation factor eIF5B on the 80S ribosome mapped by directed hydroxyl radical probing. *EMBO J.*, **26**, 3109–3123.
11. Daviter,T., Gromadski,K.B. and Rodnina,M.V. (2006) The ribosome's response to codon-anticodon mismatches. *Biochimie*, **88**, 1001–1011.
12. Cochella,L. and Green,R. (2005) An active role for tRNA in decoding beyond codon:anticodon pairing. *Science*, **308**, 1178–1180.
13. Sergiev,P.V., Lesnyak,D.V., Burakovsky,D.E., Kiparisov,S.V., Leonov,A.A., Bogdanov,A.A., Brimacombe,R. and Dontsova,O.A. (2005) Alteration in location of a conserved GTPase-associated center of the ribosome induced by mutagenesis influences the structure of peptidyltransferase center and activity of elongation factor G. *J. Biol. Chem.*, **280**, 31882–31889.
14. Dontsova,O.A. and Dinman,J.D. (2005) 5S rRNA: structure and function from head to toe. *Int. J. Biomed. Sci.*, **1**, 2–7.
15. Rakauskaite,R. and Dinman,J.D. (2006) An arc of unpaired "hinge bases" facilitates information exchange among functional centers of the ribosome. *Mol. Cell Biol.*, **26**, 8992–9002.
16. Hennelly,S.P., Antoun,A., Ehrenberg,M., Gualerzi,C.O., Knight,W., Lodmell,J.S. and Hill,W.E. (2005) A time-resolved investigation of ribosomal subunit association. *J. Mol. Biol.*, **346**, 1243–1258.
17. Warner,J.R., Vilardell,J. and Sohn,J.H. (2001) Economics of ribosome biosynthesis. *Cold Spring Harb. Symp. Quant. Biol.*, **66**, 567–574.
18. Cochella,L. and Green,R. (2004) Isolation of antibiotic resistance mutations in the rRNA by using an in vitro selection system. *Proc. Natl Acad. Sci. USA*, **101**, 3786–3791.
19. Green,R., Samaha,R.R. and Noller,H.F. (1997) Mutations at nucleotides G2251 and U2585 of 23 S rRNA perturb the peptidyl transferase center of the ribosome. *J. Mol. Biol.*, **266**, 40–50.
20. Youngman,E.M. and Green,R. (2005) Affinity purification of in vivo-assembled ribosomes for in vitro biochemical analysis. *Methods*, **36**, 305–312.
21. Polacek,N., Gomez,M.J., Ito,K., Xiong,L.Q., Nakamura,Y. and Mankin,A. (2003) The critical role of the universally conserved A2602 of 23S ribosomal RNA in the release of the nascent peptide during translation termination. *Mol. Cell*, **11**, 103–112.
22. Erlacher,M.D., Lang,K., Wotzel,B., Rieder,R., Micura,R. and Polacek,N. (2006) Efficient ribosomal peptidyl transfer critically relies on the presence of the ribose 2′-OH at A2451 of 23S rRNA. *J. Am. Chem. Soc.*, **128**, 4453–4459.
23. Ghosh,S. and Joseph,S. (2005) Nonbridging phosphate oxygens in 16S rRNA important for 30S subunit assembly and association with the 50S ribosomal subunit. *RNA*, **11**, 657–667.
24. Asai,T., Zaporojets,D., Squires,C. and Squires,C.L. (1999) An *Escherichia coli* strain with all chromosomal rRNA operons inactivated: complete exchange of rRNA genes between bacteria. *Proc. Natl Acad. Sci. USA*, **96**, 1971–1976.
25. Oakes,M., Aris,J.P., Brockenbrough,J.S., Wai,H., Vu,L. and Nomura,M. (1998) Mutational analysis of the structure and localization of the nucleolus in the yeast *Saccharomyces cerevisiae*. *J. Cell Biol.*, **143**, 23–34.
26. Wai,H.H., Vu,L., Oakes,M. and Nomura,M. (2000) Complete deletion of yeast chromosomal rDNA repeats and integration of a new rDNA repeat: use of rDNA deletion strains for functional analysis of rDNA promoter elements in vivo. *Nucleic Acids Res.*, **28**, 3524–3534.
27. Wickner,R.B. and Leibowitz,M.J. (1976) Two chromosomal genes required for killing expression in killer strains of *Saccharomyces cerevisiae*. *Genetics*, **82**, 429–442.
28. Smith,M.W., Meskauskas,A., Wang,P., Sergiev,P.V. and Dinman,J.D. (2001) Saturation mutagenesis of 5S rRNA in *Saccharomyces cerevisiae*. *Mol. Cell Biol.*, **21**, 8264–8275.
29. Ito,H., Fukuda,Y., Murata,K. and Kimura,A. (1983) Transformation of intact yeast cells treated with alkali cations. *J. Bacteriol.*, **153**, 163–168.
30. Harger,J.W. and Dinman,J.D. (2004) Evidence against a direct role for the Upf proteins in frameshifting or nonsense codon readthrough. *RNA*, **10**, 1721–1729.
31. Jacobs,J.L. and Dinman,J.D. (2004) Systematic analysis of bicistronic reporter assay data. *Nucleic Acids Res.*, **32**, e160–e170.
32. Jung,G. and Masison,D.C. (2001) Guanidine hydrochloride inhibits Hsp104 activity in vivo: a possible explanation for its effect in curing yeast prions. *Curr. Microbiol.*, **43**, 7–10.
33. Meskauskas,A., Petrov,A.N. and Dinman,J.D. (2005) Identification of functionally important amino acids of ribosomal protein L3 by saturation mutagenesis. *Mol. Cell Biol.*, **25**, 10863–10874.
34. Sachs,A.B. and Davis,R.W. (1989) The poly(A) binding protein is required for poly(A) shortening and 60S ribosomal subunit-dependent translation initiation. *Cell*, **58**, 857–867.
35. Stern,S., Moazed,D. and Noller,H.F. (1988) Structural analysis of RNA using chemical and enzymatic probing monitored by primer extension. *Methods Enzymol.*, **164**, 481–489.
36. Hansen,J.L., Moore,P.B. and Steitz,T.A. (2003) Structures of five antibiotics bound at the peptidyl transferase center of the large ribosomal subunit. *J. Mol. Biol.*, **330**, 1061–1075.
37. LaRiviere,F.J., Cole,S.E., Ferullo,D.J. and Moore,M.J. (2006) A late-acting quality control process for mature eukaryotic rRNAs. *Mol. Cell*, **24**, 619–626.
38. Nogi,Y., Vu,L. and Nomura,M. (1991) An approach for isolation of mutants defective in 35S ribosomal RNA synthesis in *Saccharomyces cerevisiae*. *Proc. Natl Acad. Sci. USA*, **88**, 7026–7030.
39. Siddiqi,I.N., Dodd,J.A., Vu,L., Eliason,K., Oakes,M.L., Keener,J., Moore,R., Young,M.K. and Nomura,M. (2001) Transcription of chromosomal rRNA genes by both RNA polymerase I and II in yeast *uaf30* mutants lacking the 30 kDa subunit of transcription factor UAF. *EMBO J.*, **20**, 4512–4521.
40. Schneider,D.A., Michel,A., Sikes,M.L., Vu,L., Dodd,J.A., Salgia,S., Osheim,Y.N., Beyer,A.L. and Nomura,M. (2007) Transcription elongation by RNA polymerase I is linked to efficient rRNA processing and ribosome assembly. *Mol. Cell*, **26**, 217–229.
41. Rose,M.D., Winston,F. and Hieter,P. (1990) *Methods in Yeast Genetics*. Cold Spring Harbor Press, Cold Spring Harbor, NY.
42. Grollman,A.P. (1967) Inhibitors of protein biosynthesis. II. Mode of action of anisomycin. *J. Biol. Chem.*, **242**, 3226–3233.
43. Inoue,T., Sullivan,F.X. and Cech,T.R. (1985) Intermolecular exon ligation of the rRNA precursor of Tetrahymena: oligonucleotides can function as 5′ exons. *Cell*, **43**, 431–437.
44. Soukup,G.A. and Breaker,R.R. (1999) Relationship between internucleotide linkage geometry and the stability of RNA. *RNA*, **5**, 1308–1325.
45. Rodriguez-Fonseca,C., Amils,R. and Garrett,R.A. (1995) Fine structure of the peptidyl transferase centre on 23 S-like rRNAs deduced from chemical probing of antibiotic-ribosome complexes. *J. Mol. Biol.*, **247**, 224–235.
46. Pestka,S. (1971) Inhibitors of ribosome functions. *Annu. Rev. Microbiol.*, **25**, 487–562.
47. Baxter-Roshek,J.L., Petrov,A.N. and Dinman,J.D. (2007) Optimization of ribosome structure and function by rRNA base modification. *PLoS One*, **2**, e174.

48. Carter,A.P., Clemons,W.M., Brodersen,D.E., Morgan-Warren,R.J., Wimberly,B.T. and Ramakrishnan,V. (2000) Functional insights from the structure of the 30S ribosomal subunit and its interactions with antibiotics. *Nature*, **407**, 340–348.
49. Dresios,J., Derkatch,I.L., Liebman,S.W. and Synetos,D. (2000) Yeast ribosomal protein L24 affects the kinetics of protein synthesis and ribosomal protein L39 improves translational accuracy, while mutants lacking both remain viable. *Biochemistry*, **39**, 7236–7244.
50. Plant,E.P., Nguyen,P., Russ,J.R., Pittman,Y.R., Nguyen,T., Quesinberry,J.T., Kinzy,T.G. and Dinman,J.D. (2007) Differentiating between near- and non-cognate codons in *Saccharomyces cerevisiae*. *PLoS ONE*, **2**, e517.
51. Sweeney,R., Yao,C.H. and Yao,M.C. (1991) A mutation in the large subunit ribosomal RNA gene of Tetrahymena confers anisomycin resistance and cold sensitivity. *Genetics*, **127**, 327–334.
52. King,T.H., Liu,B., McCully,R.R. and Fournier,M.J. (2003) Ribosome structure and activity are altered in cells lacking snoRNPs that form pseudouridines in the peptidyl transferase center. *Mol. Cell*, **11**, 425–435.
53. Palmer,E., Wilhelm,J. and Sherman,F. (1979) Phenotypic suppression of nonsense mutants in yeast by aminoglycoside antibiotics. *Nature*, **277**, 148–150.
54. Harger,J.W. and Dinman,J.D. (2003) An *in vivo* dual-luciferase assay system for studying translational recoding in the yeast *Saccharomyces cerevisiae*. *RNA*, **9**, 1019–1024.
55. Wickner,R.B. (1994) [*URE3*] as an altered URE2 protein: evidence for a prion analog in *Saccharomyces cerevisiae*. *Science*, **264**, 566–569.
56. Brunelle,J.L., Youngman,E.M., Sharma,D. and Green,R. (2006) The interaction between C75 of tRNA and the A loop of the ribosome stimulates peptidyl transferase activity. *RNA*, **12**, 33–39.
57. Samaha,R.R., Green,R. and Noller,H.F. (1995) A base pair between tRNA and 23S rRNA in the peptidyl transferase centre of the ribosome. *Nature*, **377**, 309–314.
58. Thompson,J., Kim,D.F., O'Connor,M., Lieberman,K.R., Bayfield,M.A., Gregory,S.T., Green,R., Noller,H.F. and Dahlberg,A.E. (2001) Analysis of mutations at residues A2451 and G2447 of 23S rRNA in the peptidyltransferase active site of the 50S ribosomal subunit. *Proc. Natl Acad. Sci. USA*, **98**, 9002–9007.
59. Youngman,E.M., Brunelle,J.L., Kochaniak,A.B. and Green,R. (2004) The active site of the ribosome is composed of two layers of conserved nucleotides with distinct roles in peptide bond formation and peptide release. *Cell*, **117**, 589–599.
60. Hosokawa,K., Fujimura,R.K. and Nomura,M. (1966) Reconstitution of functionally active ribosomes from inactive subparticles and proteins. *Proc. Natl Acad. Sci. USA*, **55**, 198–204.
61. Leonov,A.A., Sergiev,P.V., Bogdanov,A.A., Brimacombe,R. and Dontsova,O.A. (2003) Affinity purification of ribosomes with a lethal G2655C mutation in 23S rRNA that affects the translocation. *J. Biol. Chem.*, **278**, 25664–25670.
62. Mitra,K. and Frank,J. (2006) Ribosome dynamics: insights from atomic structure modeling into cryo-electron microscopy maps. *Annu. Rev. Biophys. Biomol. Struct.*, **35**, 299–317.
63. Moore,P.B. and Steitz,T.A. (2003) The structural basis of large ribosomal subunit function. *Annu. Rev. Biochem.*, **72**, 813–850.
64. Steitz,T.A. (2005) On the structural basis of peptide-bond formation and antibiotic resistance from atomic structures of the large ribosomal subunit. *FEBS Lett.*, **579**, 955–958.
65. Chakrabarti,S.L. and Gorini,L. (1975) A link between streptomycin and rifampicin mutation. *Proc. Natl Acad. Sci. USA*, **72**, 2084–2087.
66. Correll,C.C., Munishkin,A., Chan,Y.L., Ren,Z., Wool,I.G. and Steitz,T.A. (1998) Crystal structure of the ribosomal RNA domain essential for binding elongation factors. *Proc. Natl Acad. Sci. USA*, **95**, 13436–13441.
67. Meskauskas,A. and Dinman,J.D. (2007) Ribosomal protein L3: gatekeeper to the A-site. *Mol. Cell*, **25**, 877–888.
68. Davidovich,C., Bashan,A., Auerbach-Nevo,T., Yaggie,R.D., Gontarek,R.R. and Yonath,A. (2007) Induced-fit tightens pleuromutilins binding to ribosomes and remote interactions enable their selectivity. *Proc. Natl Acad. Sci. USA*, **104**, 4291–4296.
69. Meskauskas,A. and Dinman,J.D. (2007) Involvement of the N-terminal extension of ribosomal protein L3 in coordination of large subunit-associated functions. Submitted for publication.